RSC Advances

PAPER

View Article Online
View Journal | View Issue

Cite this: *RSC Adv.*, 2024, **14**, 3985

Alkylimidazolium-based ionic liquids with tailored anions and cations for CO_2 capture†

Abdelbagi Osman, *[a] Abobakr K. Ziyada, [b] Abdul Majeed Khan[b] and Fahd Rajab[a]

Received 6th December 2023
Accepted 22nd January 2024

DOI: 10.1039/d3ra08335g

rsc.li/rsc-advances

A systematic investigation was conducted in the present study to determine how various cations and anions affected the solubility of CO_2. To investigate the influence of different cations and anions on the solubility of CO_2, twelve ILs were synthesized, characterized, and utilized. These ILs comprised five distinct anions (dioctylsulfosuccinate [DOSS], triflouromethanesulfonate [TFMS], dodecylsulfate [DDS], 3-sulfobezoate [SBA], and benzene sulfonate [BS]), and four distinct cations (1-butyl-3-propanenitrile imidazolium [C_2CN Bim], 1-hexyl-3-propanenitrile imidazolium [C_2CN Him], 1-octyl-3-propanenitrile imidazolium [C_2CN Oim], and 1-decyl-3-propanenitrile imidazolium [C_2CN Dim]). The synthesized ILs were characterized using NMR and elemental analysis. Their moisture and halide contents were determined. The gravimetric method (MSB) was employed to determine the solubility of CO_2 at various pressures (20, 15, 10, 5, and 1 bar). In addition, the effects of temperature on the solubility of CO_2 were investigated. The constant of Henry's law (k_H) was also calculated, along with thermodynamic properties including standard enthalpy (H^0), entropy (S^0), and Gibbs free energy (G^0).

1. Introduction

Rapidly increasing industrialization in numerous nations is causing a surge in the demand for carbon dioxide capture and separation.[1,2] As a result, for the next few decades, CO_2 capture and reduction of the atmospheric CO_2 concentration will be critical.[3,4] The enhancement of natural carbon sinks, such as forests and oceans, could theoretically mitigate atmospheric CO_2 concentrations.[5] Nevertheless, the development of novel carbon capture materials is imperative from a commercial and environmental perspective, as existing concepts exhibit long-term promise but are not yet viable.[6] Aqueous amine-based solvents are used as CO_2-absorbing solvents in many industrial processes nowadays. However, numerous drawbacks exist with these solvents, such as the energy heating requirement to renew the amine. Recently, ionic liquids (ILs) have gained recognition as an alternative material to capture CO_2 and for their wide range of engineering applications.

ILs typically contain large inorganic and/or organic anions and cations and have melting points below 100 °C.[1] Different types of ILs have already been synthesized by combining various anions and cations.[1,7] ILs are a class of solvents with unique and versatile properties, including excellent solvency for a wide range of polar and nonpolar compounds, high chemical and thermal stability, negligible vapor pressure, and a broad electrochemical window. These properties make ILs well-suited for a variety of industrial and technological applications, such as biomass processing, electroplating, solar cells, lubricants, and electrolytes.[1,8,9] However, these solvents depending on their applications, may not be highly green by type 1 comparisons but may be quite green by type 2 (type 1 comparisons are process- and application-neutral, comparing solvents just on the basis of their mass, whereas type 2 comparisons are tailored to a specific application).[10] Moreover, the biodegradability and toxicity of ILs were discussed in details recently.[11]

ILs are considered as promising CO_2 capture solvents, and can physically absorb CO_2, which requires less energy to reverse as compared to chemical absorption methods.[12,13]

The main drawbacks of employing various ILs in the large-scale CO_2 are their cost and viscosity that are considered to be higher than that of traditional solvents.[14,15] Given that ILs are generally applied in diluted forms with viscosities that are not appreciably higher than water's, the high viscosity issue with ILs can be resolved.[11] The low vapor pressure, low volatility, and high stability of ILs in comparison to the solvents already in use are some of the key characteristics that facilitate their usage for CO_2 absorption. The efficiency and cost of the CO_2 absorption process are significantly affected by the high volatility and high heat degradation of conventional employed solvents such as monoethanolamine, *etc.* The fact that IL can be regenerated at 1 bar makes it a potentially economical alternative for CO_2 uptake from pre-combustion. Moreover, this would reduce the gap in

[a]*Department of Chemical Engineering, College of Engineering, Najran University, P.O. Box 1988, Najran 11001, Saudi Arabia. E-mail: aomustafa@nu.edu.sa; fmrajab@nu.edu.sa*

[b]*Department of General Studies, Jubail Industrial College, PO Box 10099, Jubail Industrial City 31961, Saudi Arabia. E-mail: taha_a@rcjy.edu.sa; abubakrkhz@yahoo.com; khan_am@rcjy.edu.sa*

† Electronic supplementary information (ESI) available. See DOI: https://doi.org/10.1039/d3ra08335g

heat transfer between operations and lower the cost of utilities involved. The ability to regenerate the ILs at 1 bar and higher temperatures potentially decrease the cost of the CO_2 capture as compared to the high cost of the conventional solvents due to significant equipment expenses connected with vacuum regeneration operations.[11,16] Previous research comparing the ILs process's cost and performance indicates that this technology is promising. Furthermore, the potential of ILs to be tailored could be potentially utilized in the development and design of inexpensive, and, thermally stable ILs with high CO_2 capture capacity and selectivity.[11] Moreover, the high degradation temperatures of ILs prevents equipment against corrosion caused by ILs reacting with impurities.[17] Finally, the tuneable nature of ILs allows scientists to design ILs with specific properties tailored to specific applications.[1]

Computational studies suggest that the anion plays a more significant role than the cation in dissolving CO_2 in ILs,[18] as the anion is a stronger base and CO_2 is a Lewis acid. However, experimental data, reveal that CO_2 is more soluble in the $[PF_6]$ anion than the $[BF_4]$ anion, implying that other factors, such as free volume, also play a role.[14] Functionalized ILs, particularly imidazolium-based functionalized ILs, have demonstrated potential for CO_2 capture.[19] Functionalizing the cation and/or anion with a reactive functional group can significantly enhance CO_2 solubility.[20] Amine-functionalized ILs absorb CO_2 by forming carbamates, while fluoroalkyl groups also exhibit a high affinity for CO_2.[6,21] Incorporating oxygen-containing functional groups, such as ether and ester groups, into the cation and anion can also increase CO_2 solubility by exploiting the ability of the electron-deficient carbon atom to attract electronegative atoms. However, it is crucial to balance the need for high CO_2 solubility with the need for easy CO_2 desorption from the IL.[22,23] Hence, large-scale industrial integration of ILs for CO_2 capture requires a comprehensive understanding of their physical and chemical properties. Therefore, experimental techniques and data development are essential for the future of practical, cost-effective, and sustainable CO_2 capture using ILs.

The current study meticulously designed IL architectures to evaluate the impact of various structural variations on CO_2 solubility. The cations were combined with various alkyl chains and functional groups, while the anions had diverse structures and functional groups. The engineered structures possess features known to enhance the CO_2-philicity of a molecule, resulting in augmented CO_2 solubility in ILs. Researchers have synthesized and investigated the CO_2 solubility in functionalized ILs.[24,25] However, no studies have examined the CO_2 solubility in imidazolium-based ILs with cations containing nitrile functionality and alkyl chains and anions containing alkyl chains incorporating a sulfonyl group, branched alkyl chain, fluoroalkyl chain, or carbonyl group.

CO_2 solubility was investigated by comparing the solubility of CO_2 in ILs with varying combinations of cations and anions, as well as ILs at the same pressure and other ILs at varying pressures. To investigate the impact of cations, anions, and pressures on CO_2 solubility, ILs containing the cations [C_2CN Bim], [C_2CN Him], [C_2CN Oim], and [C_2CN Dim] and incorporating the anions [DDS], [BS], [TFMS], [SBA], and [DOSS] were synthesized, and described.

2. Materials and methods

2.1. Materials

Analytical-grade chemicals were used to produce the ILs without further purification. Their CAS number, source, and grade denote the chemicals. Imidazole (288-32-4, 99%), acrylonitrile (107-13-1, 99%), methanol, anhydrous (67-56-1, 99.8%), 1-bromohexane (111-15-1, 99%), 1-bromodecane (112-29-8, 98%), 1-bromooctane (111-81-1, Aldrich 99%), ethyl acetate, anhydrous (141-78-6, 99.8%), acetone (67-64-1, 99.8%), diethyl ether (60-29-7, 99%), sodium dioctylsulfosuccinate (209-406-4, 98%), sodium triflouromethanesulfonate (2926-30-9, 98%), sodium benzenesulfonate (515-42-4, 97%), sodium dodecylsulfate (205-788-1, 99%), sodium 3-sulfobezoate (17625-03-5, 97%), and dichloromethane (75-09-2, 99.8%), were purchased from Sigma-Aldrich while 1-bromobutane (109-65-9, 98%) was obtained from Merck.

2.2. Synthesis

2.2.1. Alkyl nitrile imidazolium-bromide ILs [C_2CN Rim][Br]. The synthesis of the nitrile imidazolium-based ILs incorporated with different alkyl chains and sulfonate–based anions was carried out as shown in Fig. 1 and reported in the literature.[26–28] Imidazole priorly dissolved in methanol was stirred with excess of acrylonitrile and heated at 55 °C for 10 hours in a flask connected with a nitrogen gas source to produce the propanenitrile imidazole. The mixture was heated to 80 °C under reduced pressure to remove the solvent. An excess of 1-bromobutane was added to the propanenitrile imidazole, which was then heated for 48 hours at 70 °C. To produce 1-butyl-3-propanenitrile imidazolium bromide ([C_2CN Bim][Br]), the mixture was washed with ethyl acetate. The ethyl acetate was evaporated, and the resulting compound was dried in a vacuum oven for 72 hours.

By replacing 1-bromobutane with 1-bromodecane, 1-bromooctcane, and 1-bromohexane, the other nitrile imidazolium-based ILs with decyl (1-decyl-3-propanenitrile imidazolium bromide [C_2CN Dim][Br]), octyl (1-octyl-3-propanenitrile imidazolium bromide [C_2CN Oim][Br]), and hexyl (1-hexyl-3-propanenitrile imidazolium bromide [C_2CN Him][Br]) alkyl chains were synthesized using the same method as described for the synthesis of [C_2CN Bim][Br].

2.2.2. Alkyl nitrile imidazolium-based ILs incorporating sulfonated–based anions [C_2CN Rim][X]. Equimolar amounts of [C_2CN Him][Br] and sodium dodecyl sulfate were stirred together in deionized water for 48 hours for the synthesis of the ionic liquid 1-hexyl-3-propanenitrile imidazolium dodecylsulfate ([C_2CN Him][DDS]). Dichloromethane was used to extract the ILs from the mixture after water had been removed under reduced pressure, forming a precipitate.

Preparation of 1-hexyl-3-propanenitrile imidazolium benzenesulfonate [C_2CN Him][BS], 1-hexyl-3-propanenitrile imidazolium sulfobenzoic acid [C_2CN Him][SBA], and 1-hexyl-3-propanenitrile imidazolium triflouromethanesulfonate [C_2CN Him][TFMS] followed the same protocol as for the synthesis of [C_2CN Him][DDS], whereas sodium benzenesulfonate, sodium 3-sulfobezoate and sodium triflouromethanesulfonate were used instead of sodium dodecyl sulfate.

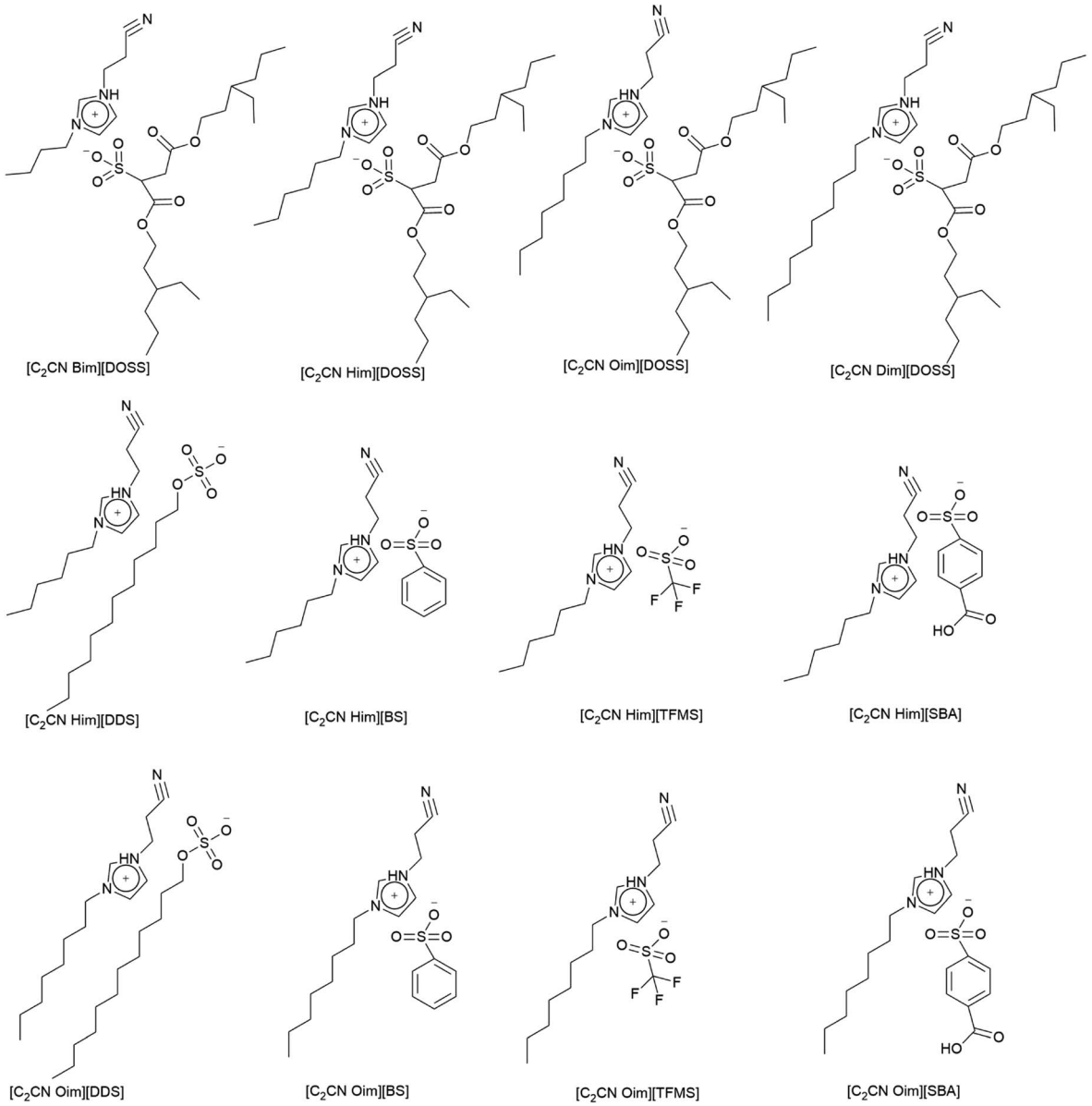

Fig. 1 Structures of the prepared ILs.

Equimolar amounts of [C_2CN Dim][Br] and sodium dioctylsuccinate were dissolved and stirred in acetone for 48 hours to produce 1-decyl-3-propanenitrile imidazolium dioctylsuccinate ([C_2CN Dim][DOSS]). The resulting solid product was removed from the mixture, washed with diethyl ether and dried under reduced pressure.

A similar procedure was followed to synthesize 1-octyl-3-propanenitrile imidazolium dioctylsuccinate [C_2CN Oim][DOSS], 1-hexyl-3-propanenitrile imidazolium dioctylsuccinate [C_2CN Him][DOSS] and 1-butyl-3-propanenitrile imidazolium dioctylsuccinate [C_2CN Bim][DOSS] by replacing [C_2CN Dim][Br] with [C_2CN Oim][Br], [C_2CN Him][Br], and [C_2CN Bim][Br], respectively.

2.3. Characterization and measurements

2.3.1. NMR and elemental analysis. A Burcher Avance 300-JEOL nuclear magnetic resonance spectrophotometer was used to determine and record the ^{1}H spectra of the synthesized ILs. Carbon, hydrogen, nitrogen, and sulfur concentrations in the produced material were measured using the elemental analyzer CHNS-932 (from LECO instruments). The manufacturer's supplied calibration chemical was used.[27]

2.3.2. Water and halide content. The water content of the prepared ILs was determined using a coulometric titrator from Mettler Toledo (Karl Fischer titrator, DL 39) equipped with the reagent CombiCoulomat fritless Karl Fischer from Merck. The ion chromatography (Metrohm Model 761 Compact IC instrument) was used to determine the halide concentration in the produced ILs. The apparatus was supplied with a Metrosep A Supp 5-150 analytical column (150 mm × 4.0 mm) and a Metrosep A Supp 4/5 guard column (d 5.0 mm × 4.0 mm). Metrodata IC Net 2.3 software was used to analyze the results.

2.3.3. Solubility of CO_2 in ILs. The gravimetric method was employed to determine the experimental solubility of CO_2 in the ILs using a magnetic suspension balance (MSB). Although this technique is frequently used to measure the solubility of gases in solids (by observing the change in weight of the sample following absorption), it is rarely used to determine the same for liquids (because evaporation can impact the final weight of the sample). Owing to the ILs' non-volatile characteristics, the gravimetric method was employed to determine their gas solvability.[29]

The magnetic suspension balance (MSB) is a versatile and precise instrument for measuring the solubility of gases in liquids. It enables real-time monitoring of mass changes, which is essential for detecting equilibrium. This is crucial because equilibrium must be attained before accurate solubility measurements can be made. Additionally, the MSB can be used to confirm the complete degassing of the initial liquid, another prerequisite for accurate results.[29]

The magnetic suspension balance (MSB) from Rubotherm, Präzisionsmesstechnik GmbH, and Bochum, Germany was used to determine the solubility of the CO_2 in the prepared ILs. The instrument employs a magnetic suspension coupling comprising an electromagnet and a suspension magnet, with the electromagnet electronically controlled to maintain the suspension magnet in a frictionless levitation state. The precision and reproducibility of the microbalance were reported to be 0.001 mg and $\pm$0.020 mg, respectively. The pressure and temperature in the measuring cell were controlled to within $\pm$0.05 bar and $\pm$0.2 °C, respectively, as reported.[30] To achieve highly accurate weight measurements, all potential environmental disturbances affecting the sample were minimized, controlled, and quantified, except for buoyancy, which was quantified and corrected using MessPro software to control the instrument and record data.

The MSB method for determining the solubility of CO_2 in the prepared ILs comprises of four main steps: blank measurement, sample drying, buoyancy correction, and solubility measurement. In the blank measurement, the empty sample container is weighed and its volume is measured. The sample is then dried to remove all water and volatile substances. The volume of the sample inside the sample container is then precisely determined using a buoyancy measurement. The measurement process began at a constant temperature and gradually increased the pressure to the desired value while being continuously monitored. The solubility measurement was considered complete when the MSB showed no further increase in mass. The apparatus, sample preparation, and measurement technique are all described in detail.[30–32]

3. Results

3.1. Characterization

The synthesized IL structures were confirmed by elemental analysis and NMR spectra. The ^{1}H NMR spectra for the ILs [C_2CN Bim][DOSS], [C_2CN Him][DOSS], [C_2CN Oim][DOSS], [C_2CN Dim][DOSS], [C_2CN Him][DDS], [C_2CN Him][BS], [C_2CN Him][TFMS], [C_2CN Him][SBA], [C_2CN Oim][DDS], [C_2CN Oim][BS], [C_2CN Oim][TFMS], and [C_2CN Oim][SBA] are presented in the ESI† along with the ^{1}H NMR spectra (Fig. SI.1–SI.5†).

Elemental analysis, water content, halide content, and purity of all prepared ILs[33] are also reported and provided in the ESI.†

3.2. Solubility of CO_2 in ILs

The maximum amount of a gas that can dissolve in a liquid at a given temperature and pressure is its solubility. At equilibrium, the rate of gas molecules entering and leaving the solution is equal. When the pressure increases, more gas molecules collide with the liquid's surface, causing the dissolved gas concentration to increase until a new equilibrium is established.[34]

Table 1 displays the mole fraction *versus* pressure results for the experimental CO_2 solubility measurements taken in the produced ILs at temperatures of 298.15 K and pressures of 1, 5, 10, 15, and 20 bar. When compared to non-functionalized imidazolium-based ILs[23,35] and ILs with amine functionality,[28,29,36] the time needed for the prepared ILs to reach their maximum solubility capacity is shorter but is still longer than the times reported for [Emim][NTf_2] and [Bmim][NTf_2].[29,37]

The solubility data in Table 1 demonstrate that the solubility of CO_2 in all of the investigated ILs positively correlates with an increase in pressure. This phenomenon can be attributed to the fact that when the pressure increases, the gas molecules are forced to dissolve into the IL solution to minimize the applied pressure to the greatest extent. Moreover, the solubility of CO_2 demonstrated a non-linear pattern with the increase in pressure across all the investigated ILs as shown in Fig. 2.

Emerging evidences suggest that CO_2 solubility in ILs is influenced by more than just interaction strength and free volume.[30,38] Seki *et al.* demonstrated that interactions alone cannot fully explain CO_2 sorption in ILs, as was previously believed, and that the strong Lewis acid-base interactions between ILs and dissolved CO_2 are not the only factor affecting CO_2 solubility.[38] Hereafter, we discuss the influence of anions and cations on CO_2 solubility.

3.3. Influence of anions on the CO_2 solubility

As demonstrated by the CO_2 solubility data in Table 1, the anion selection has a substantial effect on CO_2 solubility, which is consistent with previous research.[32,39,40] Fig. 2 and SI.6 to SI.9 (ESI†) display the isotherms of CO_2 solubility in the prepared ILs at 20, 15, 10, 5, and 1 bar. The presented figures illustrate the effect of the anion on the solubility of CO_2 in ILs containing [C_2CN Him] and [C_2CN Oim] cations at 298.15 K.

ILs with the [DOSS] anion exhibit a significantly higher affinity for carbon dioxide (CO_2) than those with the [DDS], [TFMS], [SBA], and [BS] anions due to their unique properties that enhance CO_2 solubility and affinity. These properties include carbonyl and sulfonyl functional groups, which increase the molecule's CO_2-philicity and solubility. Additionally, the long and branched alkyl chains on the DOSS anion further enhance CO_2 solubility, as demonstrated in previous studies.[41] Moreover, the molar free volume of the IL plays a significant role in determining the CO_2 solubility capacity.

Table 1 CO_2 solubility in the prepared ILs at 1, 5, 10, 15, and 20 bar as a mole fraction of CO_2 (x_{CO_2})[a]

	ILs											
x_{CO_2} (bar)	[C_2CN Bim] [DOSS]	[C_2CN Him] [DOSS]	[C_2CN Him] [TFMS]	[C_2CN Him] [SBA]	[C_2CN Him] [DDS]	[C_2CN Him] [BS]	[C_2CN Oim] [DOSS]	[C_2CN Oim] [TFMS]	[C_2CN Oim] [SBA]	[C_2CN Oim] [DDS]	[C_2CN Oim] [BS]	[C_2CN Dim] [DOSS]
1	0.053	0.070	0.035	0.032	0.0267	0.023	0.081	0.041	0.037	0.025	0.030	0.095
5	0.232	0.261	0.197	0.177	0.1595	0.144	0.264	0.214	0.192	0.173	0.157	0.315
10	0.412	0.443	0.340	0.306	0.281	0.262	0.502	0.386	0.347	0.319	0.297	0.548
15	0.562	0.598	0.460	0.414	0.378	0.350	0.657	0.506	0.455	0.426	0.384	0.701
20	0.712	0.738	0.547	0.492	0.449	0.411	0.769	0.592	0.532	0.491	0.448	0.813

[a] Standard uncertainties u of temperature, pressure and MSB (mass reading) are 0.05 K, 0.25 kPa and 0.00002 g respectively. The combined standard uncertainties of the CO_2 solubility for the ILs [C_2CN Bim][DOSS][C_2CN Him][DOSS], [C_2CN Him][TFMS], [C_2CN Him] [SBA], [C_2CN Him]DDS], [C_2CN Him][BS], [C_2CN Oim][DOSS], [C_2CN Oim][TFMS], [C_2CN Oim][SBA], [C_2CN Oim][DDS], [C_2CN Oim][BS], and [C_2CN Dim][DOSS] were 0.009, 0.014, 0.016, 0.014, 0.010, 0.013, 0.012, 0.013, 0.011, 0.010, 0.013, and 0.014 respectively.

Generally, larger anions result in a larger free volume, which provides more space for CO_2 molecules to occupy.[22] The molar-free volume of the IL was found to have a significant impact on CO_2 solubility, comparable to the anion basicity, which is a well-known key factor affecting CO_2 solubility in ILs.[6]

The fluoroalkyl groups in the [TFMS] anion interact more strongly with CO_2, making it easier for CO_2 to dissolve in the IL. This is in contrast to ILs based on the [SBA], [DDS], and [BS] anions, which do not form such strong interactions.[42,43] Two types of interactions have been identified between anions and carbon dioxide (CO_2) in ILs: acid–base interactions and CO_2–fluorine interactions. The solubility of CO_2 in ILs is positively correlated with the number of CF_3 groups in the anion.[44,45] The higher CO_2 solubility in [SBA]-based ILs than in [DDS] and [BS]-based ILs may be due to the carboxylate ion in the [SBA] anion, which enhances CO_2-philicity by increasing van der Waals interactions between CO_2 and the anion. The longer alkyl chain of the [DDS] anion increases CO_2 solubility in [DDS]-based ILs compared to [BS]-based ILs by strengthening van der Waals interactions between the gas and liquid.

3.4. Influence of cations on the CO_2 solubility

The impact of the IL cation on CO_2 solubility is examined by comparing the CO_2 solubility of synthesized ILs with same anions but different cations. The length of the side chain connecting the CN group to the imidazole ring remains constant, while the attachment of the alkyl chain to the imidazolium cation is altered. These cations were chosen because previous research has shown that adding polar and nonreactive functional groups, such as nitriles, to the cations of ILs can significantly improve CO_2/CH_4 selectivity while having little to no effect on CO_2 solubility compared to non-functionalized ILs.[20,46–49]

From the literature, it is believed that elongating the alkyl chain attached to the imidazolium cation effectively reduces the strength of the strong ion–ion interactions,[50] while a shorter side chain connecting the CN group to the IL cation reduces viscosity and melting point, and enhances interactions between the ions and CO_2 due to the weaker ionic bonding within the molecule.[51]

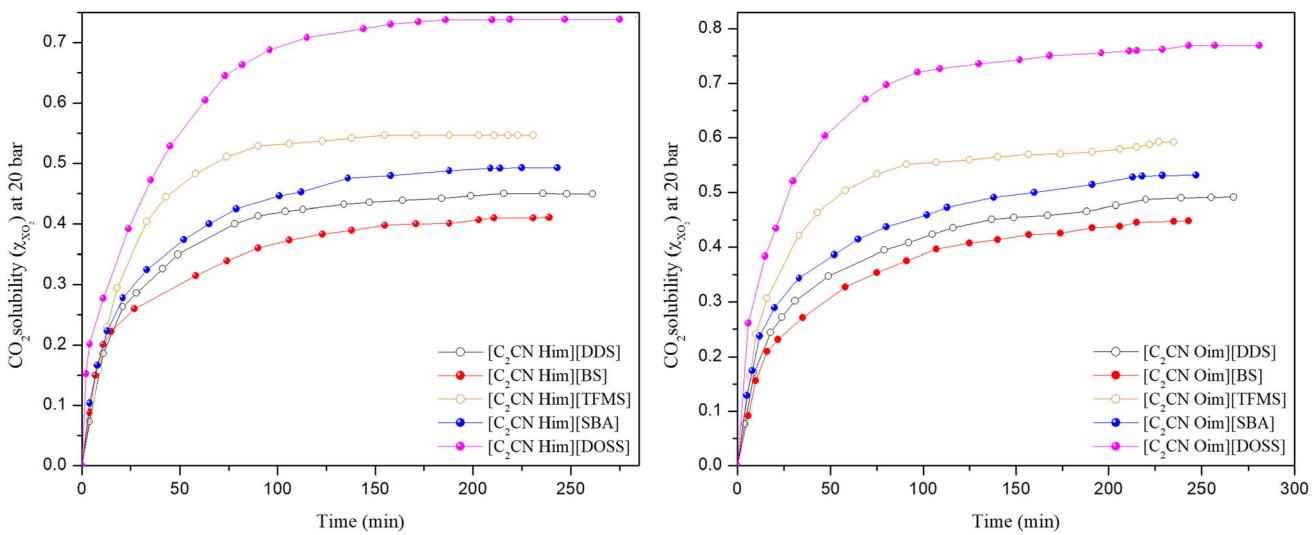

Fig. 2 CO_2 solubility in the [C_2CN Him] and [C_2CN Oim]-based ILs incorporated with [DDS], [BS], [TFMS], [SBA] and [DOSS] anions at 298.15 K at 20 bar.

However, because ILs with longer alkyl chains tend to have higher melting points,[50] and possibly higher CO_2 solubility, butyl to decyl alkyl chains were used in this study. Fig. 3 illustrates the CO_2 solubility in [DOSS]-based ILs containing [C_2CNBim], [C_2CNHim], [C_2CNOim], and [C_2CNDim] cations at 298.15 K and 5 bar.

As shown in Fig. 3, an increase in solubility occurred as a result of the cation's alkyl chain lengthening (the CO_2 solubility of [C_2CNBim] < [C_2CNHim] < [C_2CNOim] < [C_2CNDim]). As predicted, the increased free volume originating from the lengthened alkyl chain of the cation enhances the solubility of CO_2 in the ionic liquid (IL).[52] At higher pressures, the increase in solubility values with increasing alkyl chain length becomes more noticeable.[29]

In contrast to conventional ILs, where the increase in solubility is less pronounced for alkyl chains longer than 8 carbon atoms,[53] the solubility of CO_2 in ILs [C_2CNBim][DOSS], [C_2CNHim][DOSS], [C_2CNOim][DOSS], and [C_2CNDim][DOSS] does not exhibit a linear relationship with the length of the cation's alkyl chain. This may be due to the presence of the CN group on the IL side chain and the expansion of the molar volume.[24] Solid-state structural analysis of nitrile-functionalized ILs revealed that intermolecular hydrogen bonds form polymeric super-molecular networks.[24]

Table 1 shows the relationship between pressure and CO_2 solubility in ILs. When choosing an IL for CO_2 absorption, it is important to consider the process conditions, including pressure and diffusion coefficient, as well as the availability and cost of the material.

The CO_2 solubility in [C_2CNHim] and [C_2CNOim] cations with [TFMS], [SBA], [DDS], and [BS] anions is higher at 15 and 20 bar than in [C_2CNOim] with [DOSS] anions at 1, 5 and 10 bar. This demonstrates the importance of considering diffusivity when selecting a material for CO_2 absorption. CO_2 solubility in ILs increases significantly with pressure, but the rate of increase slows down and eventually plateaus. This is because Henry's sorption in the inter-ion space is responsible for the high rate of solubility at low pressure. As pressure increases, CO_2 molecules continuously occupy these spaces, preventing them from settling there.[38] To allow for additional CO_2 molecules to enter, the inter-ion gaps must be widened, which requires energy. This limits the amount of CO_2 that can enter the IL, resulting in the plateauing of solubility. Understanding CO_2 diffusivity in ILs is essential for designing and developing ionic liquid-based reaction and separation processes.

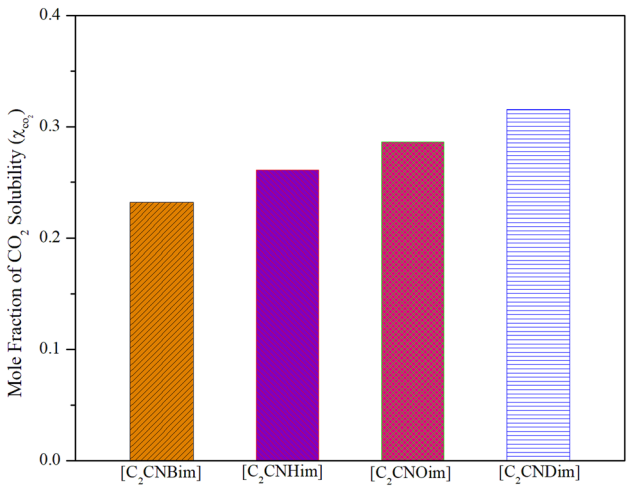

Fig. 3 Effect of cations on CO_2 solubility in the synthesized ILs at a temperature of 278.15 K and a pressure of 5 bar.

CO_2 diffusivity was estimated for the prepared ILs using a method developed by Moganty and Baltus,[54] as follows:

$$D_{CO_2} = 6.7 \times 10^5 \times \mu_{IL}^{-0.66} \times MW_{IL}^{-0.89} \times \rho_{IL}^{4.8} \times T^{-3.3} \quad (1)$$

where D_{CO_2}, μ_{IL}, MW_{IL} and T are the diffusion coefficient (m^2 s^{-1}), viscosity of IL (cP), density of IL(g cm^{-3}), molar mass of IL (g mol^{-1}) and temperature (k) respectively. The density and viscosity values used to calculate the diffusivity were published previously.[28,36,37] The calculated CO_2 diffusivity at temperatures of 298.15 to 348.15 K are reported in Table 2.

The diffusion coefficient increases with temperature, as shown in Table 2. The high viscosity of ILs with the [DOSS] anion is likely the main reason for their low diffusion coefficients. ILs with [TFMS] and [BS] anions have higher diffusion coefficients than ILs with other anions, which may be due to their lower viscosity.[27,28] Gas diffusion in ILs is partially dependent on viscosity; an increase in viscosity increases diffusion time,[29] while the dependence of diffusivity on viscosity decreases with increasing solute molar volume.[55] The CO_2 diffusivity in ILs with the [DOSS], [SBA], [DDS] and [BS] anions is low compared to that reported for the phosphonium-based IL (diffusion coefficients for [P_{66614}]-based ILs are in the range of 18.4×10^{-8} to 27.1×10^{-8}).[55] Furthermore, the diffusion coefficients of the current ILs are low compared to that reported for most of the imidazolium-based ILs such as [Hmim][BF_4], [Hmim][Tf_2N], [Omim][BF_4], and [Emim][Tf_2N].[54] These results are in a good agreement with that reported by Morgan,[56] *et al.*, Moganty, *et al.*,[54] and Camper, D., *et al.*[57] Their findings demonstrated that, while the activation energies for self-diffusion and viscosity are similar, they are considerably higher for CO_2 diffusion in ILs.[54,56,57] This comparison reveals that the molecular motion needed for carbon dioxide diffusion through an IL is significantly similar to that of self-diffusion and viscosity. The larger size of cations and anions in IL compared to CO_2 as well as the strong anion–cation coulombic interactions involved are likely the causes of the higher activation energy for self-diffusion and viscosity.[54,56,57] Furthermore, solvent viscosity is an essential component of all the formulas used for predicting gas diffusivities in ILs. To focus solely on the relationship between CO_2 diffusivity and solvent viscosity, a log–log plot of diffusivity *versus* solvent viscosity was generated using ILs with viscosities ranging across multiple orders of magnitude. The results showed that CO_2 diffusivity is generally dependent on ILs viscosity. In addition, Arshad reported that gas diffusion in an ionic liquid is dependent on its viscosity; that is, the higher the viscosity of the IL, the longer the diffusion time and, consequently, the time needed to attain equilibrium, and *vice versa*.[58] Recently, comprehensive findings on how diffusivity varies based on the type of ILs was reported.[11]

Table 2 Estimated diffusion coefficient (D_{CO_2}) of CO_2 in the synthesized ILs at different temperatures

	ILs											
Temperature, K	[C_2CN Bim][DOSS]	[C_2CN Him][DOSS]	[C_2CN Him][TFMS]	[C_2CN Him][SBA]	[C_2CN Him][DDS]	[C_2CN Him][BS]	[C_2CN Oim][DOSS]	[C_2CN Oim][TFMS]	[C_2CN Oim][SBA]	[C_2CN Oim][DDS]	[C_2CN Oim][BS]	[C_2CN Dim][DOSS]
298.15	5.18	3.24	66.64	12.49	6.35	33.85	—	25.39	8.24	—	13.50	—
308.15	9.53	5.93	111.19	21.73	11.76	56.33	3.91	42.44	14.57	6.63	25.11	2.89
318.15	16.68	10.74	179.23	38.17	21.10	98.41	7.14	73.74	25.40	12.11	43.28	5.23
328.15	28.16	18.17	270.87	65.92	36.82	155.78	11.91	120.71	42.20	20.38	73.24	8.73
338.15	48.04	29.5	418.2	112.39	59.71	229.9	18.58	189.83	71.90	31.32	121.31	13.38
348.15	77.12	46.31	626.32	181.3	90.56	309.68	29.1	277.07	125.25	49.8	193.00	21.82

3.5. Henry's constant

To design and improve separation technologies, it is essential to understand the equilibrium solubility characteristics and thermodynamic factors of any IL. The thermodynamic properties provide insight into the level of orderliness in the liquid/gas mixture and the extent of interaction between the liquid and dissolved gas.[59] The Henry's law constant was calculated using experimental data on CO_2 solubility in the studied ILs. The Gibbs free energy, enthalpy, and entropy of the solution, among other thermodynamic properties, can be determined using the Henry's law constant for CO_2 in the studied ILs.[59,60]

Henry's law constant (k_H) is a widely used metric for reporting gas solubility in liquids. It relates the equilibrium mole fraction (X_{CO_2}) of a solute in the liquid phase to its partial pressure in the gas phase.[61] Henry's law can be expressed in a variety of ways, each with its own unit and interpretation. For ILs having a very low or negligible vapor pressure, the gas phase is typically considered to be a pure gas solute.[62] Under equilibrium conditions and at infinite dilution, Henry's law constant (k_H) can be estimated using the following eqn (2), which assumes a fugacity coefficient of unity:[32,62,63]

$$k_H = \lim_{x\to 0}\left(\frac{P_{CO_2}}{x}\right) \quad (2)$$

k_H (T), denoted in units of pressure, is inversely proportional to the mole fraction (x) of gas present in the liquid, where P represents the partial pressure of the gas. The slope of the linear relationship between solubility and pressure can be applied to calculate Henry's law constants for gases that behave nearly ideally.

Under increasing pressure, the solubility of CO_2 gas in all of the investigated ILs exhibits a nonlinear trend, as shown in Fig. 4. However, when the solubility approaches zero, it becomes possible to determine the limiting slope by employing a second-order polynomial regression analysis on the available data. This approach allows for the determination of Henry's law constants.[42] Therefore, eqn (3) has been used to represent the experimental values.[6]

$$k_H = ax^2 + bx + c \quad (3)$$

Henry's law constant (k_H) at infinite dilution has been determined by solving eqn (4) using eqn (3):[63]

$$k_H = \lim_{x\to 0}\left(\frac{P_{CO_2}}{x}\right) = b \quad (4)$$

Henry's law constants for each of the ILs under investigation, are presented in Table 3. As mentioned before, the solubility of gases in a solvent is described by Henry's law constant. A decrease in this value represents an increase in the solubility of gases in the solvent.[62] Among the ILs under study, [C_2CNHim][DOSS] and [C_2CNOim][DOSS] displayed the lowest Henry's law constant values for the [C_2CNHim] and [C_2CNOim] based ILs, respectively, while [C_2CNDim][DOSS] showed the lowest Henry's law constant value for the ILs with the [DOSS] anion.

Moreover, Henry's law constant was used to study the impact of temperature on the CO_2 solubility capacity of these ILs. Henry's law constants were determined for the [DOSS] based ILs at pressures of 1, 5, 10, 15, and 20 bar and temperatures of 298.15, 313.15, 328.15, 343.15 and 358.15 K using eqn (4) and presented in Fig. 5.

The solubility of CO_2 in the IL reduces with increasing temperature, as shown in Fig. 5 is in agreement with the reported results.[64] As temperature increases, kinetic energy increases, causing ions to move faster. This reduces the interion gap and may increase the irregular distribution of ions.

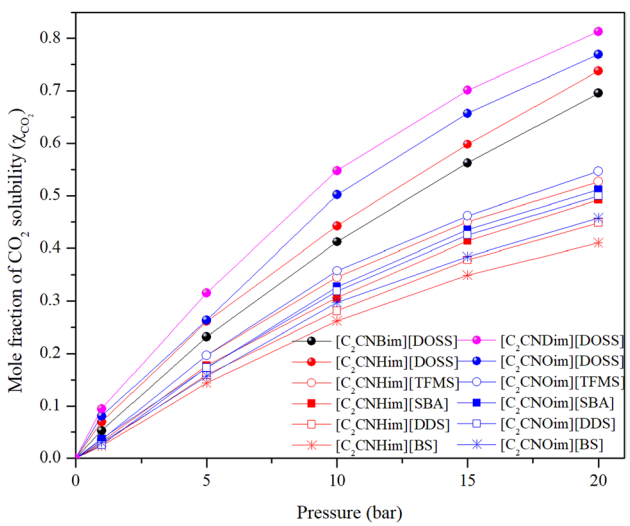

Fig. 4 Effect of pressure on CO_2 solubility in the prepared ILs at 298.15 K.

Table 3 Constants of Henry's law and correlation coefficients for the ILs under study

IL	k_H (298.15 K)	IL	k_H (298.15 K)
[C_2CN Bim][DOSS]	19.22	[C_2CN Oim][DOSS]	11.18
[C_2CN Him][DOSS]	15.69	[C_2CN Dim][DOSS]	07.47
[C_2CN Him][TFMS]	17.02	[C_2CN Oim][TFMS]	13.04
[C_2CN Him][SBA]	18.99	[C_2CN Oim][SBA]	14.37
[C_2CN Him][DDS]	20.07	[C_2CN Oim][DDS]	15.88
[C_2CN Him][BS]	21.16	[C_2CN Oim][BS]	16.61

3.6. Thermodynamic properties

The thermodynamic parameters such as standard enthalpy (ΔH^0), entropy (ΔS^0), and Gibbs free energy (ΔG^0) influence the solubility of CO_2 in ILs. At infinite dilution, the temperature dependence of Henry's law constants can be used to predict their contributions to the gas solvation process in a solvent.[32,39,40] The standard enthalpy, entropy, and Gibbs free energy of gas solubility can be derived from Henry's law constants. Eqn (5) can be used to predict the standard Gibbs free energy of a gas solution, given the standard pressure $P^0 = 1.01325$ bar and the Henry's law constant.[6]

The standard entropy of the ionic liquid/gas mixture indicates the degree of order in the mixture, while the standard enthalpy of solvation indicates the strength of the interaction between the liquid and the gas. Gibbs free energy determines whether a gas will dissolve spontaneously in a liquid, in addition to phase stability.[32,39,40,65] Additionally, negative ΔG^0 values often indicate the formation of one or more chemical complexes.[66]

The standard enthalpy, entropy, and Gibbs free energy of the gas's solubility were derived from the Henry constants. Having the standard pressure $P^0 = 1.01325$ bar and utilizing Henry's law constant,[3] eqn (5) was employed to estimate the standard Gibbs free energy of a gas solution.[6]

$$\Delta G^0 = -RT \ln\left(\frac{P^0}{k_H}\right) \quad (5)$$

Henry's law constant at infinite dilution is sometimes considered a constant and correlated to the standard enthalpy of gas dissolution. However, in other cases, ($\Delta H°$) is

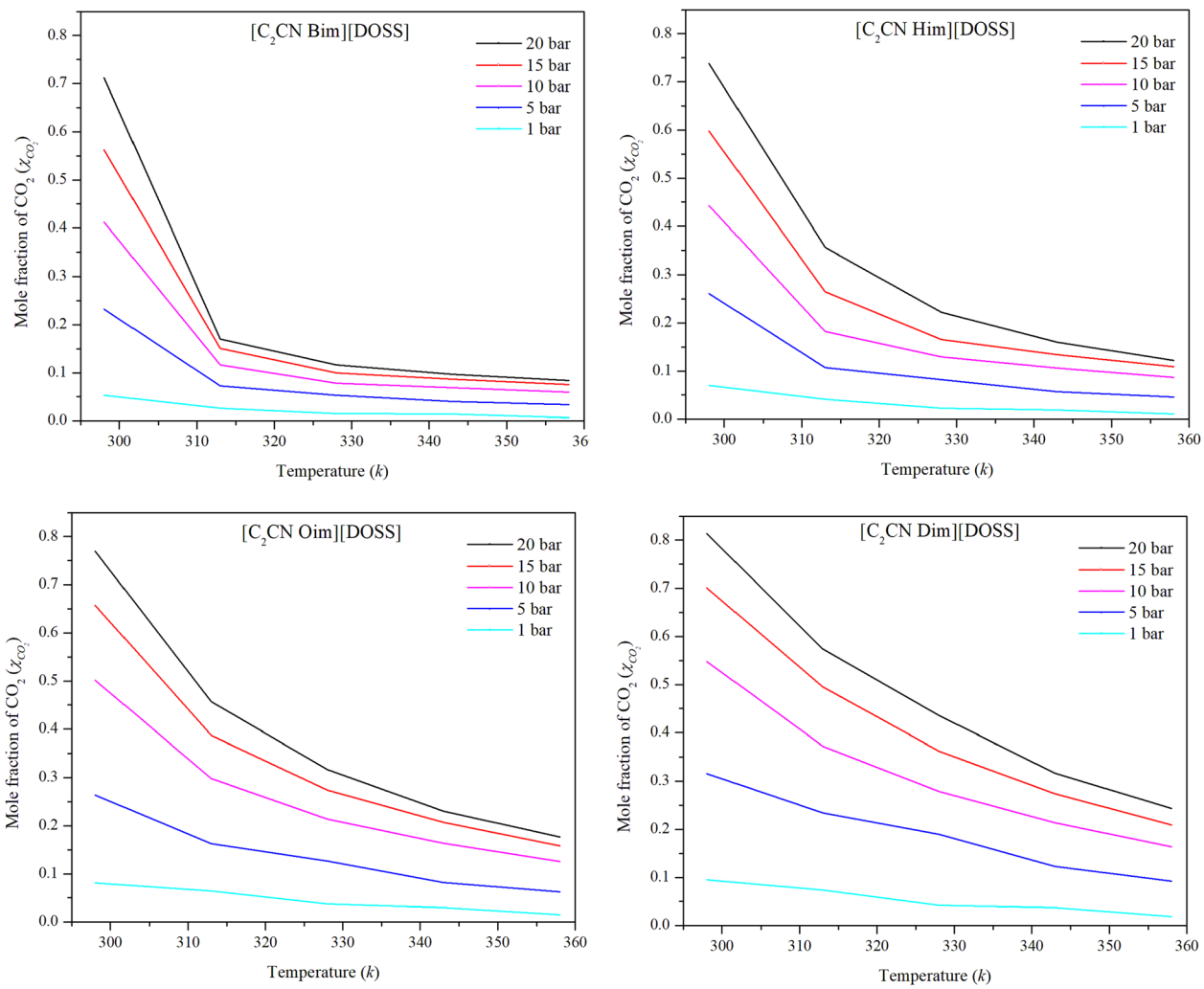

Fig. 5 Experimental data on the solubility of CO_2 in [DOSS]-based ILs at various temperatures and pressures.

Table 4 Thermodynamic properties for the solution of CO_2 in [C_2CN Rim][DOSS]

Temperature (K)	[C_2CNDim][DOSS]			[C_2CNOim][DOSS]			[C_2CNHim][DOSS]			[C_2CNBim][DOSS]		
	ΔG^0	ΔH^0	ΔS^0	ΔG^0	ΔH^0	ΔS^0	ΔG^0	ΔH^0	ΔS^0	ΔG^0	ΔH^0	ΔS^0
298.15	4.95	−17.91	−76.68	5.95	−14.38	−68.20	06.79	−10.31	−57.37	07.30	−07.55	−49.79
313.15	6.10	−17.81	−76.35	6.71	−14.87	−68.89	07.65	−11.38	−60.76	08.26	−08.59	−53.80
328.15	7.24	−17.71	−76.05	7.78	−15.31	−70.36	08.60	−12.35	−63.85	09.21	−09.53	−57.11
343.15	8.38	−17.63	−75.79	8.86	−15.71	−71.60	09.61	−13.23	−66.56	10.18	−10.39	−59.95
358.15	9.52	−17.55	−75.57	9.91	−16.07	−72.55	10.58	−14.04	−68.75	11.17	−11.18	−62.41

temperature-dependent rather than constant for relatively large temperature ranges.[6] By plotting the inverse of absolute temperature against the natural logarithm of Henry's constant ($\ln k_H$), the molar enthalpy change during gas solubility can be approximated using eqn (6) as follows:[6]

$$\Delta H^0 = R\left(B + \frac{2C}{T}\right) \quad (6)$$

Eqn (7) was utilized to calculate the standard entropy.[6]

$$\Delta S^0 = \left(\frac{\Delta H^0 - \Delta G^0}{T}\right) \quad (7)$$

Table 4 presents the Gibbs free energy, standard enthalpy, and entropy of the CO_2 solution in the [DOSS]-based ILs at various temperatures. The positive values of ΔG^0 that were previously reported indicate the CO_2 solubility in the prepared ILs. The negative values of ΔH^0 confirm the dissolution of CO_2 in the ILs, with a decrease in magnitude from moderately strong acid–base bonds at 298 K to weak acid-base bonds at 343 K, consistent with the previous reports.[63]

The enthalpy of liquids is lower than that of gases, so negative enthalpy changes occur when gases condense. Therefore, the magnitude and sign of the enthalpy of mixing determine the overall partial enthalpy change for solvation. Gas–liquid mixtures with greater solubility typically undergo a negative partial molar enthalpy change due to the dominant enthalpy of condensation.[67] A greater negative enthalpy indicates a stronger interaction between the ionic liquid (IL) and CO_2.[68] In contrast, temperature had a relatively small impact on CO_2– [C_2CNDim][DOSS] interaction. The negative solvation enthalpies further support the exothermic nature of the solvation process. The correlation between temperature and ΔG^0 suggests that more energy is needed for the CO_2 solvation process as the temperature rises. The observed solvation entropy values can be explained by the structuring effect, which is caused by the unique interactions between the charged centers of the IL and the solute.[63]

4. Conclusion

A series of nitrile-based imidazolium ILs incorporating different alkyl chains and sulfonated-based anions were synthesized in order to investigate the effect of the structure, pressure, and temperature on the CO_2 solubility. The solubility of CO_2 demonstrated a non-linear pattern with the increase in pressure among the investigated ILs. The CO_2 solubility in the prepared ILs showed the order; [DOSS] > [TFMS] > [SBA] > [DDS] > [BS] for the anions and [C_2CNDim] > [C_2CNOim] > [C_2CNHim] > [C_2CNBim] for the cations. The synthesized [DOSS]-based ILs showed higher CO_2 solubility and low diffusivity whereas the [BS]-based ILs showed lower CO_2 solubility and higher diffusivity. For Henry's law constant, [C_2CN Dim][DOSS] and [C_2CN Him][BS] showed the lowest and highest values respectively. The CO_2 solubility in the synthesized ILs showed a non-spontaneous process as indicated by the thermodynamic results.

Data availability statement

Any additional data will be available upon request.

Author contributions

Conceptualization, A. K. Z. and A. O.; methodology, A. K. Z., and A. M. K.; validation, A. K. Z., F. R., and A. M. K.; formal analysis, A. O., and M. M; investigation, F. R. and A. K. Z.; resources, A. K. Z. and A. O.; data curation, A. K. Z., and A. O.; writing—original draft preparation, A. K. Z and A. O.; writing—review and editing, A. K. Z., A. M. K., and F. R.; visualization, A. K. Z. and A. O.; supervision, A. K. Z.; project administration, A. O.; funding acquisition, A. O. All authors have read and agreed to the published version of the manuscript.

Conflicts of interest

The authors declare no conflict of interest.

Acknowledgements

The authors are thankful to the Deanship of Scientific Research at Najran University for funding this work under the Distinguished Researcher Program grant code (NU/DRP/SERC/12/54).

References

1 E. Torralba-Calleja, J. Skinner and D. Gutiérrez-Tauste, *J. Chem.*, 2013, **2013**, 1–16.
2 R. Baker, *Ind. Eng. Chem. Res.*, 2002, **41**, 1393–1411.

3 S. D. Kenarsari, D. Yang, G. Jiang, S. Zhang, J. Wang, A. G. Russell, Q. Wei and M. Fan, *RSC Adv.*, 2013, **3**, 22739–22773.
4 Q. Wang, J. Luo, Z. Zhong and A. Borgna, *Energy Environ. Sci.*, 2011, **4**, 42–55.
5 Y. Liang, MSc, Tsinghua University, 2003.
6 F. Karadas, M. Atilhan and S. Aparicio, *Energy Fuels*, 2010, **24**, 5817–5828.
7 J. D. Holbrey and K. Seddon, *Clean Prod. Process.*, 1999, **1**, 223–236.
8 K. R. Seddon, *Nat. Mater.*, 2003, **2**, 363–365.
9 A. E. Jimenez, M. D. Bermudez, F. J. Carrion and G. Martinez-Nicolas, *Wear*, 2006, **261**, 347–359.
10 P. G. Jessop, *Green Chem.*, 2011, **13**, 1391–1398.
11 W. F. Elmobarak, F. Almomani, M. Tawalbeh, A. Al-Othman, R. Martis and K. Rasool, *Fuel*, 2023, **344**, 128102.
12 M. J. Earle and K. R. Seddon, *Pure Appl. Chem.*, 2000, **72**, 1391–1398.
13 K. E. Gutowski, *Physical Sciences Reviews*, 2018, **3**(5), 20170191.
14 M. Ramdin, T. W. de Loos and T. J. Vlugt, *Ind. Eng. Chem. Res.*, 2012, **51**, 8149–8177.
15 D. Hospital-Benito, J. Lemus, C. Moya, R. Santiago, V. Ferro and J. Palomar, *Chem. Eng. J.*, 2021, **407**, 127196.
16 F. O. Ochedi, J. Yu, H. Yu, Y. Liu and A. Hussain, *Environ. Chem. Lett.*, 2021, **19**, 77–109.
17 M. Kosmulski, J. Gustafsson and J. B. Rosenholm, *Thermochim. Acta*, 2004, **412**, 47–53.
18 M. Pan, Y. Zhao, X. Zeng and J. Zou, *Energy Fuels*, 2018, **32**, 6130–6135.
19 H. S. Schrekker, M. P. Stracke, C. M. L. Schrekker and J. Dupont, *Ind. Eng. Chem. Res.*, 2007, **46**, 7389–7392.
20 F. Ding, X. He, X. Luo, W. Lin, K. Chen, H. Li and C. Wang, *Chem. Commun.*, 2014, **50**, 15041–15044.
21 Y. S. Sistla and V. Sridhar, *J. Mol. Liq.*, 2021, **325**, 115162.
22 J. Bara, C. Gabriel, T. Carlisle, D. Camper, A. Finotello, D. Gin and R. Noble, *Chem. Eng. J.*, 2009, **147**, 43–50.
23 X. Zhang, Z. Liu and W. Wang, *AIChE J.*, 2008, **54**, 2717–2728.
24 D. Zhao, Z. Fei, R. Scopelliti and P. J. Dyson, *Inorg. Chem.*, 2004, **43**, 2197–2205.
25 Q. Zhang, Z. Li, J. Zhang, S. Zhang, L. Zhu, J. Yang, X. Zhang and Y. Deng, *J. Phys. Chem. B*, 2007, **111**, 2864–2872.
26 A. K. Ziyada, C. D. Wilfred, M. A. Bustam, Z. Man and T. Murugesan, *J. Chem. Eng. Data*, 2010, **55**, 3886–3890.
27 A. K. Ziyada, M. A. Bustam, T. Murugesan and C. D. Wilfred, *New J. Chem.*, 2011, **35**, 1111–1116.
28 A. K. Ziyada, M. A. Bustam, C. D. Wilfred and T. Murugesan, *J. Chem. Eng. Data*, 2011, **56**, 2343–2348.
29 M. W. Arshad and K. Thomsen, MSc, Technical University of Denmark, 2009.
30 A. K. Ziyada and C. D. Wilfred, *J. Chem. Eng. Data*, 2018, **63**, 3672–3683.
31 M. S. R. Shahrom, C. D. Wilfred and A. K. Z. Taha, *J. Mol. Liq.*, 2016, **219**, 306–312.
32 M. Gonzalez-Miquel, J. Bedia, C. Abrusci, J. Palomar and F. Rodriguez, *J. Phys. Chem. B*, 2013, **117**, 3398–3406.
33 M. Shiflett and A. Yokozeki, *J. Phys. Chem. B*, 2007, **111**, 2070–2074.
34 J. C. Kotz, P. Treichel and J. R. Townsend, *Chemistry & Chemical Reactivity*, Brooks/Cole Pub Co, 2008.
35 J. L. Anthony, J. L. Anderson, E. J. Maginn and J. F. Brennecke, *J. Phys. Chem. B*, 2005, **109**, 6366–6374.
36 A. K. Ziyada and C. D. Wilfred, *J. Chem. Eng. Data*, 2014, **59**, 1232–1239.
37 A. K. Ziyada and C. D. Wilfred, *J. Chem. Eng. Data*, 2014, 1385–1390.
38 T. Seki, J. D. Grunwaldt and A. Baiker, *J. Phys. Chem. B*, 2008, **113**, 114–122.
39 A. M. Tagiuri, *Studies of Solubility of CO_2 in Ionic Liquids, Kinetics, and Heat of Reactions of CO_2 in Promising Cyclic Amines*, The University of Regina, Canada, 2019.
40 S. N. V. K. Aki, B. R. Mellein, E. M. Saurer and J. F. Brennecke, *J. Phys. Chem. B*, 2004, **108**, 20355–20365.
41 L. A. Blanchard, PhD, University of Notre Dame, 2000.
42 G. Yu, S. Zhang, X. Yao, J. Zhang, K. Dong, W. Dai and R. Mori, *Ind. Eng. Chem. Res.*, 2006, **45**, 2875–2880.
43 E. D. Bates, R. D. Mayton, I. Ntai and J. H. Davis, *J. Am. Chem. Soc.*, 2002, **124**, 926–927.
44 J. Bara, D. Camper, D. Gin and R. Noble, *Acc. Chem. Res.*, 2009, **43**, 152–159.
45 T. Sarbu, T. J. Styranec and E. J. Beckman, *Ind. Eng. Chem. Res.*, 2000, **39**, 4678–4683.
46 J. A. Schott, C.-L. Do-Thanh, W. Shan, N. G. Puskar, S. Dai and S. M. Mahurin, *Green Chemical Engineering*, 2021, **2**, 392–401.
47 C. Wu, T. P. Senftle and W. F. Schneider, *Phys. Chem. Chem. Phys.*, 2012, **14**, 13163–13170.
48 X. Liu, K. E. O'Harra, J. E. Bara and C. H. Turner, *J. Phys. Chem. B*, 2021, **125**, 3665–3676.
49 S. D. Hojniak, I. P. Silverwood, A. L. Khan, I. F. Vankelecom, W. Dehaen, S. G. Kazarian and K. Binnemans, *J. Phys. Chem. B*, 2014, **118**, 7440–7449.
50 D. Zhao, MSc, Xinan Petroleum University, 2007.
51 R. P. Swatloski, PhD, University of Alabama, 2005.
52 W. Ren, B. Sensenich and A. Scurto, *J. Chem. Thermodyn.*, 2010, **42**, 305–311.
53 D. Almantariotis, T. Gefflaut, A. Pa dua, J. Coxam and M. Costa Gomes, *J. Phys. Chem. B*, 2010, **114**, 3608–3617.
54 S. S. Moganty and R. E. Baltus, *Ind. Eng. Chem. Res.*, 2010, **49**, 9370–9376.
55 B. E. Gurkan, T. R. Gohndrone, M. J. McCready and J. F. Brennecke, *Phys. Chem. Chem. Phys.*, 2013, **15**, 7796–7811.
56 D. Morgan, L. Ferguson and P. Scovazzo, *Ind. Eng. Chem. Res.*, 2005, **44**, 4815–4823.
57 D. Camper, C. Becker, C. Koval and R. Noble, *Ind. Eng. Chem. Res.*, 2006, **45**, 445–450.
58 M. W. Arshad, *Measuring and Thermodynamic Modeling of De-Mixing CO_2 Capture Systems*, Technical University of Denmark, 2014.
59 J. Huang, A. Riisager, R. Berg and R. Fehrmann, *J. Mol. Catal. A: Chem.*, 2008, **279**, 170–176.

60 J. Anthony, E. Maginn and J. Brennecke, *J. Phys. Chem. B*, 2002, **106**, 7315–7320.
61 A. Henni, P. Tontiwachwuthikul and A. Chakma, *Can. J. Chem. Eng.*, 2005, **83**, 358–361.
62 L. M. G. Sánchez, PhD, Eindhoven University of Technology, 2008.
63 H. W. Pennline, D. R. Luebke, K. L. Jones, C. R. Myers, B. I. Morsi, Y. J. Heintz and J. B. Ilconich, *Fuel Process. Technol.*, 2008, **89**, 897–907.
64 G. Wang, W. Hou, F. Xiao, J. Geng, Y. Wu and Z. Zhang, *J. Chem. Eng. Data*, 2011, **56**(4), 1125–1133.
65 P. Carvalho, V. Álvarez, I. Marrucho, M. Aznar and J. Coutinho, *J. Supercrit. Fluids*, 2010, **52**, 258–265.
66 M. Koel, *Proc. Est. Acad. Sci., Chem.*, 2000, **49**, 145–155.
67 A. Finotello, J. E. Bara, D. Camper and R. D. Noble, *Ind. Eng. Chem. Res.*, 2008, **47**, 3453–3459.
68 M. Muldoon, S. Aki, J. Anderson, J. Dixon and J. Brennecke, *J. Phys. Chem. B*, 2007, **111**, 9001–9009.